FEBS Letters 587 (2013) 989–993

journal homepage: www.FEBSLetters.org

Structural basis for pH gating of plant aquaporins

Anna Frick, Michael Järvå, Susanna Törnroth-Horsefield *

Department of Chemistry and Molecular Biology, University of Gothenburg, P.O. Box 462, SE-405 30 Gothenburg, Sweden

ARTICLE INFO

Article history:
Received 3 January 2013
Revised 14 February 2013
Accepted 15 February 2013
Available online 27 February 2013

Edited by Julian Schroeder

Keywords:
Membrane protein
Aquaporin
Plasma membrane intrinsic protein
pH gating
X-ray crystallography

ABSTRACT

Plants have evolved to cope with fluctuations in water supply by gating their water channels known as aquaporins. During flooding, a rapid drop of cytosolic pH due to anoxia leads to a simultaneous closure of the aquaporins in the plasma membrane. The closing mechanism has been suggested to involve a conserved histidine on cytosolic loop D. Here we report the crystal structure of a spinach aquaporin at low pH, revealing for the first time the structural basis for how this pH-sensitive histidine helps to keep the aquaporin in a closed state.

1. Introduction

Plants depend on their ability to regulate water flow across their cellular membranes in response to environmental stress such as drought, flooding or high salinity [1]. This task is performed by aquaporins, a well-conserved family of membrane protein channels which allow water to pass along osmotic or hydrostatic pressure gradients. Aquaporins can be found in most living species and share a common tetrameric fold with each monomer functioning as an individual water channel, comprising six transmembrane helices and two half-membrane spanning helices (Fig. 1A).

In order to maintain proper water homeostasis plants express a larger number of aquaporin isoforms than for example mammals and yeast. In the model plant *Arabidopsis thaliana,* 35 isoforms have been identified compared to only 13 in humans [2]. In addition, plants are able to rapidly fine-tune water transport rates through individual aquaporins by gating. Plant aquaporins have been shown to be gated by phosphorylation [3–5], divalent cations [6–8] and pH [1,6–11].

The phenomenon of pH gating of plant aquaporins occurs in response to flooding. During flooding, a rapid drop of cytosolic pH due to anoxia causes closure of the aquaporins situated in the plant plasma membrane (plasma membrane intrinsic proteins, PIPs) [11]. The first clues to the molecular mechanism behind this event came from studies on PIPs from *Arabidopsis thaliana*. In this study, a fully conserved histidine in the intracellular loop D was identified as the main pH sensor. By mutating this residue of AtPIP2;2 to alanine, aspartic acid and lysine respectively and assaying the water transport in oocytes it was concluded that protonation of this histidine at low pH triggers a simultaneous closure of PIPs. The role of this histidine in pH gating of plant aquaporins has been confirmed by further studies on PIP2;1 from *Arabidopsis thaliana*[8] as well as PIP2;1 from tobacco [1].

We have previously solved the crystal structure of the spinach aquaporin SoPIP2;1 in both closed and open conformations revealing how a conformational change of intracellular loop D is responsible for gating of the channel. In the closed structure, loop D caps the water channel from the intracellular side, inserting a hydrophobic residue, Leu 197 into the channel opening (Fig. 1A) [12]. The closed conformation is stabilized through interactions with an N-terminal divalent cation binding site. Using this structural framework, we proposed a mechanism for how gating can be achieved in response to phosphorylation of two highly conserved serines, Ser115 in loop B and Ser274 in the C-terminus, or by pH through protonation of His193 in loop D.

The proposed gating mechanism involves an interaction between His193 and the divalent cation binding site, occupied by Cd^{2+} in the closed structure, but presumed to bind Ca^{2+} *in vivo*. The Cd^{2+}-ion is ligated by two well-conserved residues, Asp28 and Glu31, at a short N-terminal helix as well as by two water molecules (Fig. 1B). In the closed structure at pH 8, His193 is pointing away from the Cd^{2+}-site, however a putative flip of the side chain

Abbreviations: AQP, aquaporin; PIP, plasma membrane intrinsic protein

* Corresponding author.
E-mail address: tornroth@chem.gu.se (S. Törnroth-Horsefield).

0014-5793/$36.00
http://dx.doi.org/10.1016/j.febslet.2013.02.038

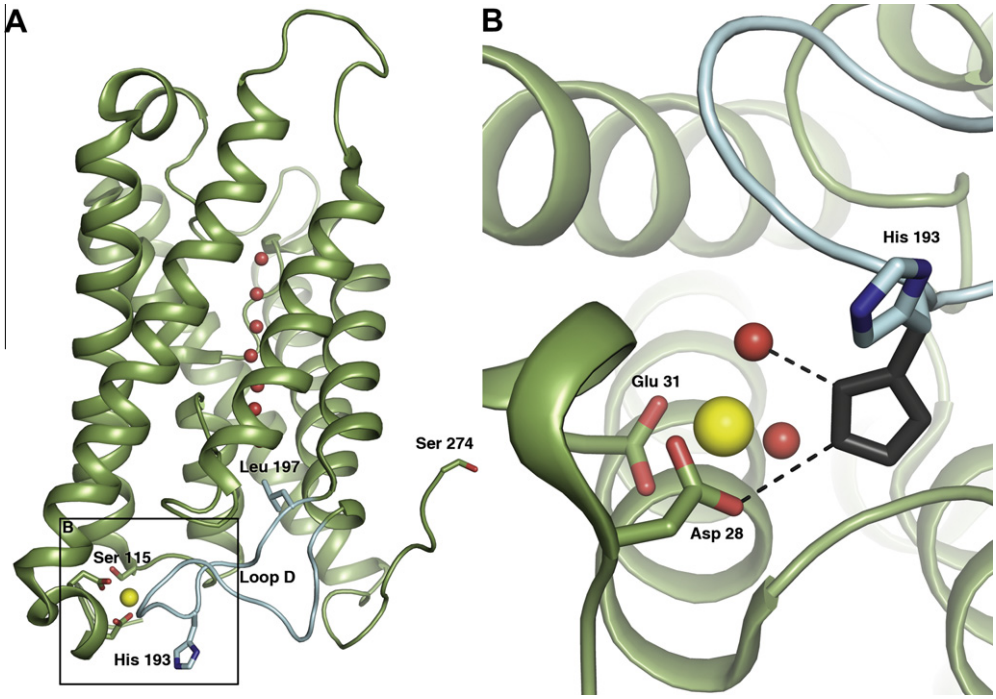

Fig. 1. Proposed gating mechanism for SoPIP2;1. (A) Overview of SoPIP2;1 in the closed conformation at pH8 (pdb code 1Z98). Interactions between Loop D (blue) and a Cd^{2+}-binding site at the N-terminus inserts a hydrophobic plug indicated by Leu 197, thereby occluding the water conducting pore. The Cd^{2+}-ion and water molecules in the water conducting channel are shown as yellow and red spheres respectively. Residues involved in gating by phosphorylation (Ser 115 and Ser 274) as well as gating by pH (His 193) are indicated. (B) Close-up view of His 193. In the protonated state, an alternative rotamer of the His193 side-chain (grey) may be adopted which is within hydrogen bonding distance of Asp28.

would allow for an interaction to occur with Asp28, thus stabilizing loop D in the closed conformation.

Here we present the 3.1 Å crystal structure of SoPIP2;1 at pH 6 without Cd^{2+} revealing for the first time His193 participating in an interaction which maintains the water channel in a closed state. This gives important new insights into the structural mechanism behind pH gating of plant aquaporins.

2. Results and discussion

2.1. Structural determination of SoPIP2;1 at pH 6

The aim of the present study was to elucidate the structural basis for pH-gating of SoPIP2;1 and in particular the role of His193. To this end, we crystallized and solved the structure of SoPIP2;1 at pH 6 in the absence of Cd^{2+}. Under these conditions, SoPIP2;1 crystallized in a space group lacking the fourfold symmetry otherwise typically associated with aquaporin structures, allowing structural differences to be observed between monomers within the aquaporin tetramer. The structure was solved to 3.1 Å resolution by molecular replacement using a tetramer of the closed structure of SoPIP2;1 at pH 8 as the search model. After iterative rounds of refinement and manual rebuilding into composite omit maps to reduce model-bias, an R-factor of 23.7% and free R-factor of 24.3% was obtained (Table 1).

Table 1
Data collection and refinement statistics.

Data collection	
Space group	$P2_12_12$
Cell dimensions	
a, *b*, *c* (Å)	178.23, 104.19, 66.52
α, β, γ (°)	90, 90, 90
Resolution (Å)[a]	104–3.1 (3.27–3.1)
R_{merge}[a]	0.099 (0.667)
$I/\sigma I$[a]	11.1 (1.6)
Completeness[a]	98.2 (99.6)
Redundancy[a]	3.9 (4.0)
Refinement	
Resolution (Å)[a]	90–3.1 (3.18–3.1)
No. of reflections[a]	21 484 (1605)
R_{work}/R_{free}[a]	0.237/0.243 (0.357/0.381)
No. of atoms	
Protein	7281
Ion	12
Water	1
Average B-factors	
Protein	98.19
Ion	171.45
Water	81.05
R.m.s. deviations	
Bond lengths (Å)	0.008
Bond angles (°)	1.584
Ramachandran values (%)	
Favoured	87.4
Allowed	12.6
Outliers	0
Protein Data Bank accession code	4IA4

[a] Values for highest resolution shell are given in parantheses.

2.2. The structure of SoPIP2;1 at pH 6 is closed

The overall structure of SoPIP2;1 at pH 6 is very similar to the closed structure at pH 8 with loop D adopting the closed conformation (Fig 2A). The two structures overlay with a root mean square deviation of 0.501 Å for 924 Cα-atoms (Fig. S1 online). As calculated by the program HOLE [13] the water-conducting pore narrows to a diameter of 1.5 Å at Leu197 on the cytosolic side, verifying that channel is in a closed state. Hydrogen bonds between Gly94 and Arg190 as well as Asp191 and Ser36 help maintain loop D in the closed conformation (Fig. 2B). Interestingly, the residue corresponding to Asp191 has been proposed to cooperate

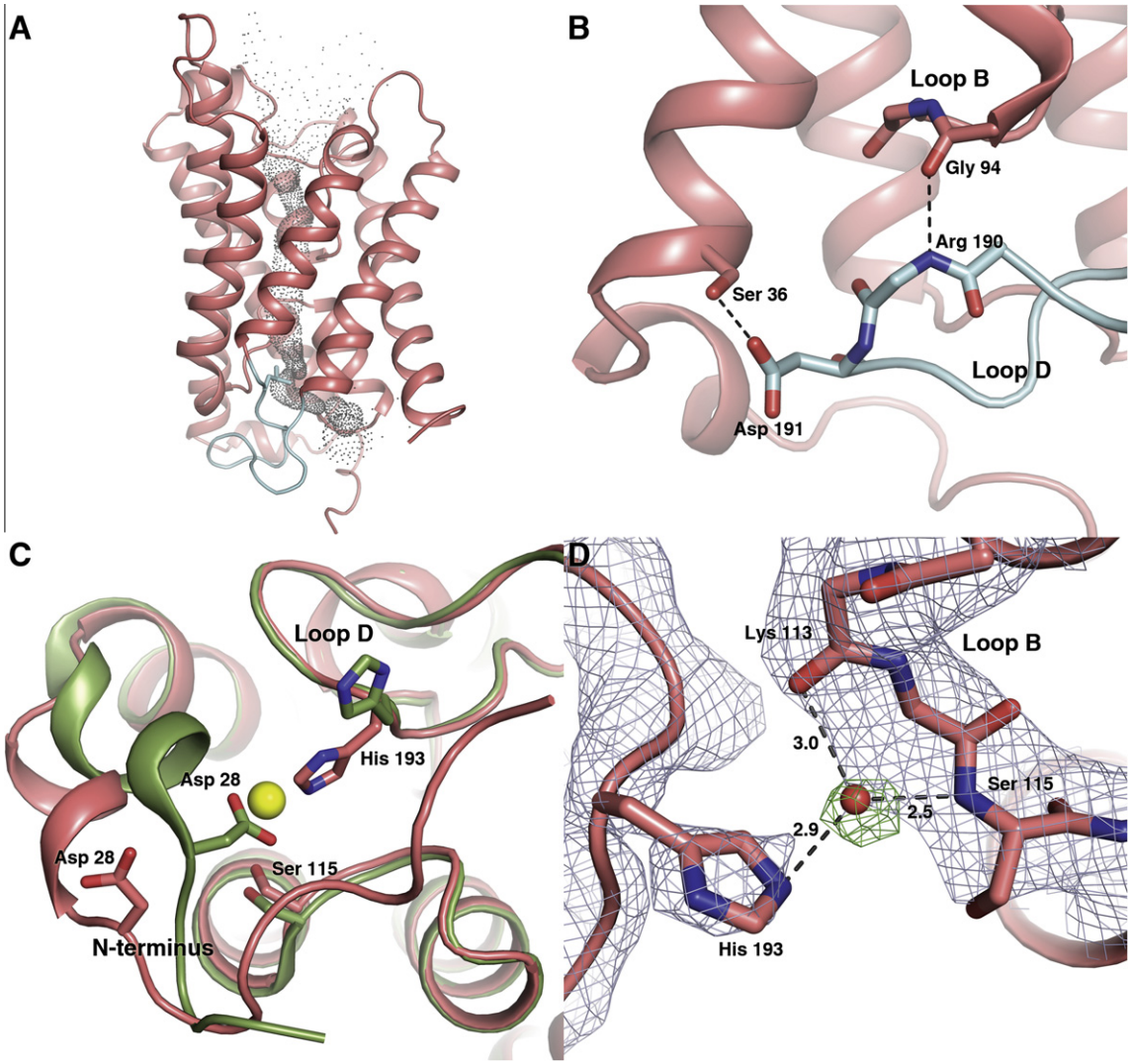

Fig. 2. Crystal structure of SoPIP2;1 at pH 6. (A) Overall structure of SoPIP1;1 at pH 6 showing the closed conformation of loop D (blue). The output from HOLE indicating the boundaries of the water conducting channel are shown as small grey spheres. At Leu197, the channel narrows to 1.5 Å which is too narrow for water to pass through. (B) Interactions stabilizing loop D (blue) in the closed conformation. Hydrogen bonds are indicated by dotted lines. (C) Comparison of the closed structures of SoPIP2;1 at pH6 and pH8 respectively. The structure at pH6 (pink) is overlaid on the structure at pH 8 (green). The yellow sphere represents Cd^{2+} from the structure at pH8. In the structure at pH6, His193 has flipped towards the Cd^{2+} binding site, but since the N-terminus has been displaced due to the absence of Cd^{2+}, no interaction between the two can be seen. (D) $2f_o$–f_c electron density map (blue, contoured at 1σ) showing the interaction between the flipped side chain of His193 and loop B. A positive peak in the f_o–f_c map (green, contoured at 3σ) compatible with a water molecule (red sphere) is present between His193 and the backbone of loop B, making hydrogen bonds between them possible. Distances are shown in Å.

with the pH-sensitive histidine in AtPIP2;1 [8]. However, since both these interactions are also present in the closed structure at pH8 they are not likely to be responsible for the pH-sensitivity of the water transport through SoPIP2;1.

2.3. His193 interacts with loop B to stabilize the closed conformation

Based on the closed structure of SoPIP2;1 at pH8, we proposed that at low pH, His193 would interact with the N-terminal Cd^{2+}-binding site, thus stabilizing loop D in the closed conformation. The proposed mechanism involved a flip of the protonated His193 side chain to allow for a hydrogen bond with the Cd^{2+}-ligand Asp28 (Fig. 1B). In our new structure at pH 6, the proposed flip of the His193 side chain can be clearly seen in one of the monomers (monomer C) of the tetramer (Fig. 2C). However, due to the absence of Cd^{2+}, the short N-terminal helix which harbours the Cd^{2+}-binding site has moved away, displacing Asp28 up to 4 Å. Instead, the flipped side chain of His193 is in close proximity of loop B and the second Cd^{2+}-ligand Glu31. A clear positive peak at 3.0 σ in the difference electron density map can be seen between His193 and loop B. This peak is compatible with a water molecule, connecting the side chain of His193 with the backbone of loop B through hydrogen bonds with the amide nitrogen of Ser115 and the carbonyl oxygen of Lys113 (Fig 2D). Difference electron density peaks of similar magnitude can also be seen for water molecules in the water-conducting channel, indicating that although modelling of waters at this resolution must be done with great care, the data supports the presence of water molecules at well-defined locations (Fig. S2 online).

The interaction between His193 and loop B via the water molecule is involved in stabilizing loop D in the closed conformation, showing for the first time the structural basis for the involvement of this residue in pH-gating of plant aquaporins. At pH 6, it is not surprising that the flip of the histidine side chain cannot be seen in all monomers. The imidazole side chain of histidine has a pK_a of approximately 6.0 and a mixed protonation state between the

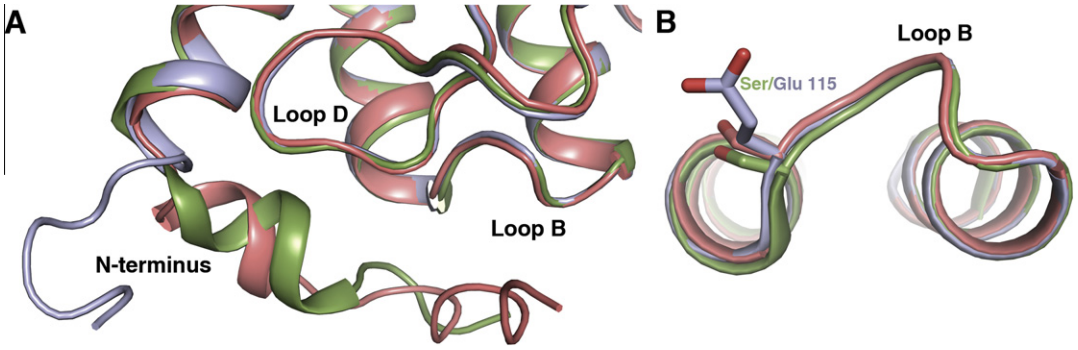

Fig. 3. Comparison of the N-terminus and loop B in SoPIP2;1 structures. Overlay of the closed structures of SoPIP2;1 at pH6 (pink) and pH8 (green) with the structure of the S115E mutant (blue, pdb code 3CLL). (A) View of the N-terminus showing how the phospho-mimetic S115E mutation causes an extension of TM helix 1 and disruption of the divalent cation binding site. (B) Close-up of loop D showing that although the N-terminus undergoes significant structural rearrangement in the S115E mutant, the main chain structure of loop B remains unaffected.

monomers in the tetramer can therefore be expected. In monomer A, His193 seems to be protonated, but since it is participating in crystal contacts it is not available for interactions with loop B.

Because of the somewhat limited resolution, it is not immediately obvious from the structure why His193 needs to be in the double protonated state for this interaction to occur. However in all earlier structures of SoPIP2;1 which has been at pH > 6, His193 is seen adopting a conformation which does not allow for any interaction with loop B or with the N-terminus as previously suggested. Together with the significant biochemical evidence that pin-points this residue as responsible for the pH-gating, this strongly suggests that the conformation seen here is indeed a result of the histidine being in a protonated state.

The observation that all monomers are closed, regardless of the conformation of His193 can be explained by the fact that channel closure is also triggered by dephosphorylation of Ser115 and Ser274 [4]. As with our previous structures of SoPIP2;1 [12,14], the electron density map reveals that the protein is in the dephosphorylated state, thereby pushing the equilibrium of the open-to-closed transition towards the closed conformation of the channel regardless of the pH.

2.4. Implications for gating by phosphorylation and Ca^{2+}

Although central to gating of plant aquaporins by phosphorylation and strictly conserved in all PIPs [4], the involvement of Ser115 in pH gating has not been predicted previously. In the closed structure of SoPIP2;1 at pH8, Ser115 hydrogen bonds to the Cd^{2+}-ligand Glu31. Molecular dynamics simulations have shown that when this residue is phosphorylated, the Cd^{2+}-binding site is perturbed, releasing loop D from its interactions with the N-terminus, thereby allowing it to adopt an open conformation. This was further supported by the crystal structure of the phosphomimetic S115E mutant of SoPIP2;1 which revealed a complete disruption of the Cd^{2+}-binding site and an extension of TM helix 1 [14] (Fig 3A). While the serine to glutamate replacement had a dramatic effect on the structure of the N-terminus and the Cd^{2+}-binding site, the backbone structure of loop B remained unaffected (Fig 3B). Since His193 interacts with only backbone atoms of Ser115, loop D would be able to adopt the closed conformation regardless of whether Ser115 is phosphorylated or not, allowing for an immediate response to a rapid drop in cytosolic pH.

It could be argued that the observed interaction between His193 and Ser115 is due to the absence of Cd^{2+} in the crystal (corresponding to Ca^{2+} *in vivo*) rather than the lower pH. However, while Cd^{2+} is lacking in all monomers, His193 is only seen participating in this interaction in one of these, thereby strongly suggesting that the reason for this interaction lies in the protonation state of the histidine rather than the absence of a divalent cation. This is further supported by the fact that in the SoPIP2;1 S115E mutant structure which also lacks Cd^{2+} this interaction is missing as well [14].

2.5. Combined effect of Ca^{2+} and low pH during flooding

Our previously suggested pH gating mechanism of PIPs involved an interaction between the conserved histidine on loop D and the Cd^{2+}-binding site. The fact that we in the absence of Cd^{2+} see an interaction with loop B instead does not necessarily contradict this. Plants respond to oxygen deprivation with not only a drop in cytosolic pH but this can also be accompanied with an increase in cytosolic Ca^{2+}-concentration [15–17]. Thus, a combined effect of low pH and Ca^{2+} on the water transport through PIPs seems plausible. Verdoucq et al. showed that in AtPIP2;1, mutation of Asp28 as well as Glu31 to alanine lead to reduced pH-sensitivity, supporting a role for the divalent cation binding site in pH gating of PIPs [8]. It is probable that in the presence of Ca^{2+} and at low pH, loop D is maintained in a closed conformation via interactions with the divalent cation binding site as previously suggested (Fig. 1B).

With the structure of SoPIP2;1 at pH 6, we provide for the first time structural evidence for the involvement of His193 on cytosolic loop D in pH gating. Furthermore we have discovered a novel interaction between His193 and loop B showing how stabilization of loop D in the closed conformation can be achieved at low pH in the absence of Ca^{2+}. This helps complete the emerging picture of how distinct biochemical signals such as phosphorylation, pH and Ca^{2+} all act on the same structural elements to gate plant aquaporins in response to environmental stress.

3. Methods

3.2. Protein overproduction and purification

Functional wild type SoPIP2;1 was overproduced in the methylotrophic yeast *Pichia pastoris* as described previously [18]. Overproduction and purification protocols are detailed in Supplementary Information. Briefly, washed membranes were solubilized in 5% octyl-β-D-glucopyranoside (β-OG) at room temperature. SoPIP2;1 was purified in a two step manner using Resource S (GE Healthcare) cation exchange followed by gelfiltration using a Superdex 200 300/10HK column (GE Healthcare) equilibrated with 20 mM Tris–HCl, pH 7.5, 100 mM NaCl, 1% β-OG. SoPIP2;1 was concentrated to ~15 mg/mL using a VivaSpin concentrator with 10 000 MWCO (Sartorius Stedim Biotech GmbH).

3.3. Crystallisation

Crystals were obtained by the hanging drop vapour diffusion technique. Protein solution containing 15 mg/mL SoPIP2;1 incubated with 5 mM $HgCl_2$ was mixed with reservoir solution in a 1:1 ratio and left to equilibrate at 4 °C.

The reservoir solution contained 22% PEG400, 100 mM sodium citrate pH 6.0, 50 mM NaCl and 20 mM $MgCl_2$. Rod-shaped crystals grew over a period of a few months. After soaking in mother liquor containing 28% PEG 400 for cryo-protection, crystals were flash frozen in liquid nitrogen.

3.4. Data collection and structural determination

X-ray diffraction data were collected at 100 K on beamline ID14-4 of the European Synchtrotron Radiation Facility (Grenoble, France). The structure was solved by molecular replacement using a tetramer of the closed structure of SoPIP2;1 at pH 8 as the model (pdb accession code 1Z98). Iterative rounds of refinement and rebuilding into composite omit maps resulted in a model with an R-factor and free R-factor of 23.7% and 24.3% respectively. Data, refinement and model statistics are shown in Table 1. For details on data processing, refinement and model building, see Supplementary information online. The structure has been deposited in the Protein Data Bank with accession code 4IA4.

Acknowledgements

This work was supported by the Swedish Research Council as a grant to S.T-H.

Appendix A. Supplementary data

Supplementary data associated with this article can be found, in the online version, at http://dx.doi.org/10.1016/j.febslet.2013.02.038.

References

[1] Fischer, M. and Kaldenhoff, R. (2008) On the pH regulation of plant aquaporins. J. Biol. Chem. 283, 33889–33892.
[2] Maurel, C. (2007) Plant aquaporins: novel functions and regulation properties. FEBS Lett. 581, 2227–2236.
[3] Maurel, C., Kado, R.T., Guern, J. and Chrispeels, M.J. (1995) Phosphorylation regulates the water channel activity of the seed-specific aquaporin alpha-TIP. EMBO J. 14, 3028–3035.
[4] Johansson, I., Karlsson, M., Shukla, V.K., Chrispeels, M.J., Larsson, C. and Kjellbom, P. (1998) Water transport activity of the plasma membrane aquaporin PM28A is regulated by phosphorylation. Plant Cell 10, 451–459.
[5] Guenther, J.F., Chanmanivone, N., Galetovic, M.P., Wallace, I.S., Cobb, J.A. and Roberts, D.M. (2003) Phosphorylation of soybean nodulin 26 on serine 262 enhances water permeability and is regulated developmentally and by osmotic signals. Plant Cell 15, 981–991.
[6] Gerbeau, P., Amodeo, G., Henzler, T., Santoni, V., Ripoche, P. and Maurel, C. (2002) The water permeability of *Arabidopsis* plasma membrane is regulated by divalent cations and pH. Plant J. 30, 71–81.
[7] Alleva, K., Niemietz, C.M., Maurel, C., Parisi, M., Tyerman, S.D. and Amodeo, G. (2006) Plasma membrane of *Beta vulgaris* storage root shows high water channel activity regulated by cytoplasmic pH and a dual range of calcium concentrations. J. Exp. Bot. 57, 609–621.
[8] Verdoucq, L., Grondin, A. and Maurel, C. (2008) Structure-function analysis of plant aquaporin AtPIP2;1 gating by divalent cations and protons. Biochem. J. 415, 409–416.
[9] Leitao, L., Prista, C., Moura, T.F., Loureiro-Dias, M.C. and Soveral, G. (2012) Grapevine aquaporins: gating of a tonoplast intrinsic protein (TIP2;1) by cytosolic pH. PLoS ONE 7, e33219.
[10] Sutka, M., Alleva, K., Parisi, M. and Amodeo, G. (2005) Tonoplast vesicles of *Beta vulgaris* storage root show functional aquaporins regulated by protons. Biol. Cell 97, 837–846.
[11] Tournaire-Roux, C., Sutka, M., Javot, H., Gout, E., Gerbeau, P., Luu, D.T., Bligny, R. and Maurel, C. (2003) Cytosolic pH regulates root water transport during anoxic stress through gating of aquaporins. Nature 425, 393–397.
[12] Törnroth-Horsefield, S., Wang, Y., Hedfalk, K., Johanson, U., Karlsson, M., Tajkhorshid, E., Neutze, R. and Kjellbom, P. (2006) Structural mechanism of plant aquaporin gating. Nature 439, 688–694.
[13] Smart, O.S., Neduvelil, J.G., Wang, X., Wallace, B.A. and Sansom, M.S. (1996) HOLE: a program for the analysis of the pore dimensions of ion channel structural models. J. Mol. Graph. 14 (354–360), 376.
[14] Nyblom, M., Frick, A., Wang, Y., Ekvall, M., Hallgren, K., Hedfalk, K., Neutze, R., Tajkhorshid, E. and Törnroth-Horsefield, S. (2009) Structural and functional analysis of SoPIP2;1 mutants adds insight into plant aquaporin gating. J. Mol. Biol. 387, 653–668.
[15] Gout, E., Boisson, A., Aubert, S., Douce, R. and Bligny, R. (2001) Origin of the cytoplasmic pH changes during anaerobic stress in higher plant cells. Carbon-13 and phosphorous-31 nuclear magnetic resonance studies. Plant Physiol. 125, 912–925.
[16] Subbaiah, C.C., Bush, D.S. and Sachs, M.M. (1994) Elevation of cytosolic calcium precedes anoxic gene expression in maize suspension-cultured cells. Plant Cell 6, 1747–1762.
[17] Sedbrook, J.C., Kronebusch, P.J., Borisy, G.G., Trewavas, A.J. and Masson, P.H. (1996) Transgenic AEQUORIN reveals organ-specific cytosolic Ca^{2+} responses to anoxia and *Arabidopsis thaliana* seedlings. Plant Physiol. 111, 243–257.
[18] Karlsson, M., Fotiadis, D., Sjovall, S., Johansson, I., Hedfalk, K., Engel, A. and Kjellbom, P. (2003) Reconstitution of water channel function of an aquaporin overexpressed and purified from *Pichia pastoris*. FEBS Lett. 537, 68–72.